67º congresso 2012 abm
67th abm international congress
ISSN 1516-392X

D.C TRIODE PLASMA NITRIDING AND PVD COATING OF ULTRA-LOW CARBON (ULC) STEEL: EFFECTS ON CORROSION BEHAVIOR COMPARED TO GALVANIZED STEELS[1]

Carlos Alberto Llanes Leyva[2]
Geralda Cristina Durães de Godoy[3]
Monica Schvartzman[4]
Antônio César Bozzi[5]

Abstract
The characterization and corrosion behavior of Ti-stabilized Ultra-Low Carbon (ULC) steel after surface modification by D.C Triode Plasma Nitriding (DC-TPN) and sequential coating with CrAlN by Electron Beam Plasma Assisted Physical Vapor Deposition (EB-PAPVD) were investigated. Manufacturing processes were described. The ULC steel substrate, the nitrided steel and the corresponding CrAlN duplex were studied. Results from corrosion tests of plasma-modified systems were compared to those from uncoated, electro-galvanized and galvannealed ULC steel sheets. Results indicate that it is feasible to manufacture duplex Ti-ULC steel via DC-TPN and EB-PAPVD with actual improvement of the corrosion resistance. Potentiodynamic curves clearly showed a shift to higher corrosion potentials and lower corrosion current intensity from the untreated ULC substrate to the duplex system.
Keywords: Ti-stabilized ultra-low carbon steel; Corrosion resistance; Duplex coating.

NITRETAÇÃO A PLASMA TRIODO D.C E RECOBRIMENTO PVD DE AÇO ULTRA-BAIXO CARBONO (UBC): INFLUÊNCIA NO COMPORTAMENTO À CORROSÃO COMPARADA À DO AÇO GALVANIZADO

Resumo
Neste trabalho foi investigado o comportamento à corrosão de aço ultra-baixo carbono estabilizado com Ti, após Nitretação a Plasma Triodo D.C (DC-TPN) e recobrimento seqüencial com CrAlN a Plasma por Deposição Física de Vapor com Feixe de Elétrons (EB-PAPVD). Os processos de fabricação são descritos. O substrato de aço UBC, o aço nitretado e o correspondente sistema dúplex com CrAlN foram estudados. Os resultados de ensaios de corrosão dos sistemas modificados a plasma foram comparados com o aço não tratado e com o aço galvanizado e eletrogalvanizado. Esses resultados indicam que é viável a fabricação de sistema dúplex em UBC-Ti via DC-TPN e EB-PAPVD com ganho na resistência à corrosão. As curvas potenciodinâmicas claramente se deslocaram para potenciais de corrosão mais altos e intensidades de corrosão menores, para o sistema dúplex comparado ao substrato não tratado ou galvanizado.
Palavras-chave: Aço ultra-baixo carbono; Resistência à corrosão; Recobrimento duplex.

[1] *Technical contribution to 67th ABM International Congress, July, 31th to August 3rd,2012, Rio de Janeiro, RJ, Brazil.*
[2] *Mechanical Engineer. Dr. Professor, Faculdade UCL, Serra, ES, Brazil - carlosleyva@ucl.br*
[3] *Metallurgy and Mines Engineering. Dr. Professor, PPGEM, Universidade Federal de Minas Gerais (UFMG), Brazil.*
[4] *Chemical Engineer. Dr. Researcher, Center for Development of Nuclear Technology (CDTN), MG, Brazil.*
[5] *Metallurgical Engineer. Dr. Professor, DEM, Universidade Federal do Espírito Santo (UFES), Brazil.*

ISSN 1516-392X

1 INTRODUCTION

In the present work the results from corrosion tests of plasma-modified (nitrided and duplex) systems are compared to those from uncoated, electro-galvanized and galvannealed ULC steel sheets. Open Circuit Potential (*OCP*) tests were performed; the corrosion behavior was evaluated via electrochemical potentiodynamic tests in aerated chloride-containing solution (3.5% NaCl). Polarization curves were investigated from -2.5 V to +1.5 V, beyond the pitting potential for CrAlN coatings which lies between 0.6V and 0.8V depending on the Al/Cr ratio[1]. Corrosion parameters were measured and compared: E_{OCP} (V); *Icorr*; (µA/cm^2); *Ecorr* (V). SEM post-corrosion studies were conducted and the corrosion modes - from general corrosion in uncoated steel to pitting in coated systems - are discussed. Characterization of chemical composition, microstructure, phases, and surface roughness were conducted. Coating thickness for the coated systems was measured by calotest.

Over the past few years the range of applications of ultra-low carbon (ULC) steels has spread widely. These steels show low yield strength and excellent formability. They have also been employed as Zn coated sheets either hot-dip galvanized (GI), galvannealed (GA) or electrogalvanized (EG) for improving the protection of the steel substrate against corrosion.[2]

Plasma Assisted Physical Vapor Deposition (PAPVD) could be a potential coating method for enhancing both mechanical resistance and corrosion resistance of low strength alloys.[3,4]However, when deposited onto low mechanical resistance alloys PAPVD coatings may undergo premature failure if the substrate plastically deforms under heavy load. An extra load support is necessary for hard coatings to perform satisfactorily. Combined treatments involving plasma nitriding and PAPVD coating have been used to improve the load-bearing capacity of hard films.[5] Other plasma thermochemical treatments such as nitriding, carburizing, carbonitriding and post-oxidation have also been employed to improve corrosion and wear resistance, as well as to increase the surface hardness and fatigue life.[6]

Development of chromium aluminum ternary nitride (CrAlN) by incorporating Al in transition binary CrN thin films has been intensively investigated in recent years.[1,7] It has been reported that CrAlN film can form both Al_2O_3 and Cr_2O_3 protective layers at the surface, preventing further diffusion of oxygen into the bulk film and thereby increasing film corrosion resistance. CrAlN also exhibits lower thermal conductivity than CrN, good tribological properties and high hardness; so it is a promising coating candidate for diverse applications.

Corrosion behavior of uncoated ULC-steels has been recently documented in technical literature.[8-10] More detailed information on corrosion behavior of galvanized ULC steels is also available.[8,11,12] Some research work has been done regarding the corrosion resistance of low carbon steels (AISI 1010 and 1020) which underwent surface modification via PAPVD processes.[13-15] However, no reference was found up to this date regarding corrosion behavior of ULC steel surface modified via plasma nitriding and sequential coating.

This work is focused on the characterization and corrosion behavior of Ti-stabilized Ultra-Low Carbon (Ti-ULC) steel after surface modification by D.C Triode Plasma Nitriding (DC-TPN) and sequential coating with CrAlN by Electron Beam Plasma Assisted Physical Vapor Deposition (EB-PAPVD). The response to corrosion of the plasma treated ULC steel samples is compared to the corrosion behavior of galvannealed GA-ULC and electrogalvanized EG-ULC steels. The corrosion

ISSN 1516-392X

properties of the target materials were studied via polarization experiments in aerated chloride-containing solution (3.5% NaCl). The morphology of the corroded samples was analyzed using scanning electron microscopy (SEM).

2 MATERIALS AND METHODS

2.1 Sampled Materials and Plasma Surface Modifications

Sample ID, nomenclature and manufacturing conditions for the different systems under investigation in this work are listed in Table 1.

Table 1. Sample ID, nomenclature and manufacturing conditions for different systems under investigation

Description and manufacturing conditions	Nomenclature
As received: Uncoated, untreated, cold rolled Ti-stabilized ULC steel	ULC
Plasma nitrided Ti-ULC steel: D.C Triode Plasma Nitriding at 500°C for 2 hrs	ULC-TPN
Plasma Duplex Ti-ULC steel: D.C. Triode Plasma Nitriding at 500°C for 2 hrs followed by EBPAPVD CrAlN coating	Duplex-ULC
Galvannealed Ti-ULC steel: Full hard sheets galvannealed via continuous line in 0.10 wt% Al+Zn bath at 440°C, re-heated to 565°C, and strain hardened	ULC-GA
Electro-galvanized Ti-ULC steel: Annealed sheets processed in continuous Gravitel line	ULC-EG

Table 2 lists the substrate chemical composition for the Ti-ULC steel sampled for plasma modification processes, as well as for similar Ti-ULC steel sheets before industrial continuum treatments of galvannealing and electro galvanization. Substrate chemical compositions were investigated by combustion method with LECO CS-444 and LECO TC-136 analyzers (for determining C, S and N contents), and optical emission spectroscopy with ARL-3460 analyzer for the remaining elements.

Table 2. Chemical composition in at. % for the Ti stabilized ULC steel substrates taken for plasma modification processes (A), and for galvannealing and electro galvanization (B)

Elements (wt. %)								
ULC substrate	C	Mn	Si	P	S	Al	Ti	Nb
A	0.0025	0.0817	0.0099	0.0096	0.0090	0.0476	0.0639	0.0002
B	0.0023	0.0700	0.0100	0.0092	0.0110	0.0240	0.0550	0.0020
ULC substrate	N	B	Cu	Ni	Cr	Mo	Sn	Fe (Bal.)
A	0.0015	0.0002	0.0081	0.0131	0.0110	0.0014	0.0003	99.74
B	0.0027	0.0001	0.0100	0.0131	0.0100	0.0000	0.0010	99.77

For comparison, ULC substrate samples were studied in the as-received condition. The material was also studied after D.C Triode Plasma Nitriding (DC-TPN), and finally as a duplex system. The duplex system was manufactured via DC-TPN and sequential coating with CrAlN by Electron Beam Plasma Assisted Physical Vapor Deposition (EB-PAPVD). Galvannealed and electrogalvanized samples were taken as subjects for comparative study.
All the Ti-ULC sampled materials (either uncoated or galvanized) were manufactured under standard industrial conditions by Usiminas S.A, a Brazilian steel company.

ISSN 1516-392X

Plasma modification processes were conducted by Tecvac Ltd., U.K. Mirror polished Ti-ULC steel samples were ultrasonically cleaned in a fully automated cleaning line to remove any surface contamination. After cleaning, samples were surface modified by D.C. Triode Plasma Nitriding (DC-TPN) and PAPVD CrAlN coating. D.C. triode plasma nitriding was carried out in a Tecvac IP70L system. For duplex samples, CrAlN coating was deposited by Electron Beam Plasma-Assisted Physical Vapour Deposition (EB-PAPVD) using a Tecvac IP90L twin e-beam system. In order to improve coating adhesion, a thin interlayer of high-purity Cr was deposited prior to CrAlN coating. Before any of the above surface modification processes, samples were subjected to a 5 minutes sputter clean stage in Ar glow discharges. For all plasma processes, bulk temperature of the substrate was continuously monitored using a thermocouple mounted on a dummy sample.

2.2Corrosion Tests and Characterization Techniques

Electrochemical tests were carried out on Ti-ULC steel systems in a non-deaerated solution of 3.5% NaCl. The electrochemical measurements were performed in a three-electrode electrochemical flat cell, at room temperature (Figure 1). The reference electrode was Ag/AgCl (3M KCl) and a platinum wire was used as the auxiliary electrode. The measurements were performed using an Autolab® potentiostat system (PGSTAT20).

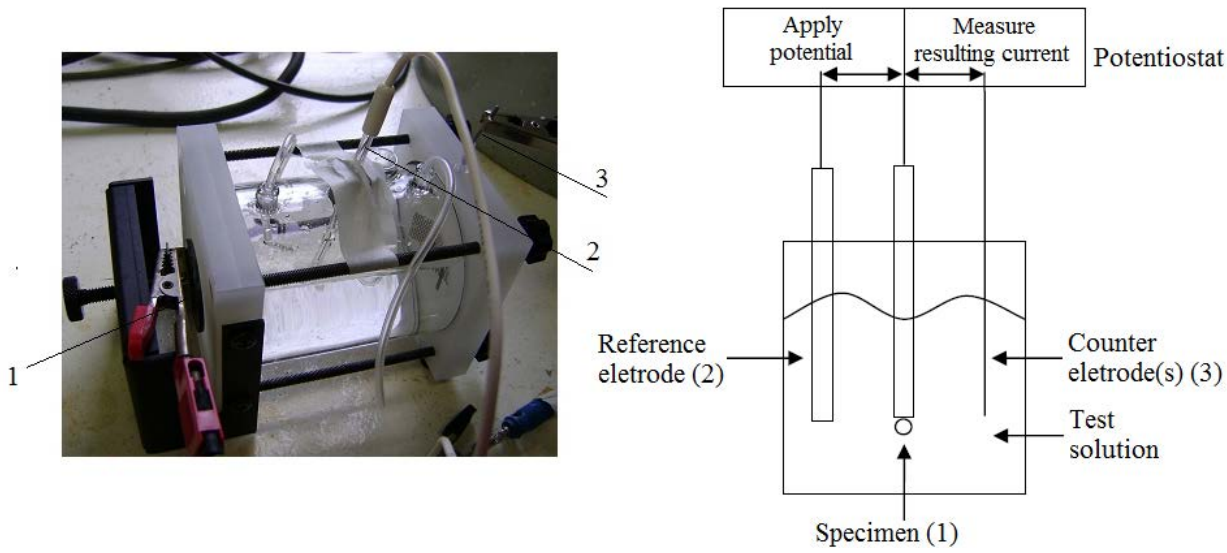

Figure 1. Arrangement of the electrochemical corrosion test cell and related instrumentation.

Different electrochemical techniques were used to compare the corrosion behavior of the samples. The open circuit potential was recorded vs. time during 24h. The potentiodynamic polarization tests were performed according to ASTM G5-94[16] The anodic potentials were applied after holding under open-circuit conditions for about 5 minutes. The potential was swept from -2.2 V below the corrosion potential up to +1.4 V. The scan rate was 0.6 mV/s. Some characteristic electrochemical parameters were measured and compared.

ISSN 1516-392X

For the polarization resistance measurements, samples were kept in *OCP* conditions for 55 minutes, and the corresponding E_{OCP} value was measured. Then, external potential was applied from -50 V to +50 V around the measured *OCP* value at a scan rate 0.167 mV/s (0.6 V/h). Linearization of the *E – I* curve was conducted for calculating the polarization resistance Rp (Ω*cm^2).
Characterization of chemical composition, microstructure, phases, and surface roughness were conducted. X-Ray diffraction analyses were carried out using a Philips PW3020 diffractometer in a Bragg–Brentano configuration ($\theta/2\theta$) and Cu$K\alpha$ radiation source (λ = 0.154056 nm, 40kV, 20 mA). The detector (2θ) was scanned from 3° to 120° at a slow rate of 0.02°/s. Phase identification was accomplished by comparison against diffraction standards from the International Center for Diffraction Data (ICDD). Stylus profilometry (Talysurf CLI 1000, Taylor-Hobson) was used for topographical study of the initial, non-corroded, samples. Scanning electron microscopy (SEM) was performed using a Zeiss EVO 40XVP with integrated IXRF EDS analyzer in corroded (top) samples as well as in fracture cross-section surfaces. Post-corrosion studies via SEM were performed and the corrosion modes (from severe general corrosion in untreated steel to general corrosion and pitting in coated systems) were identified and discussed.
For the Duplex-ULC, galvannealed and electro-galvanized samples the coating thickness was measured by calotests[17,18] in a TE66 Micro-Scale Abrasion Tester (Phoenix), computing the mean value over three replicates. Coating was also studied in SEM micrographs of the transverse section.

3 RESULTSAND DISCUSSION

The surface roughness of the samples measured by stylus profilometry before corrosion tests is illustrated in Figure2 (please note that different scales were used from Figures 2a to 2d). The numerical values for the amplitude and statistical parameters of the initial surface roughness are shown in Table 3. The surface roughness of the as-received ULC steel was significantly reduced by metallographic grinding and polishing.
Plasma nitriding did not essentially change the polished surface topography, as evidenced by the ULC-TPN sample. Sequential coating of the plasma nitrided steel (Duplex-ULC) increased the maximum peak and valley heights - as localized non-uniformities - but essentially did not change the *Sa* and *Sq* parameters of the nitrided surface. The ULC-GA sample showed the highest roughness values. Both galvannealed ULC-GA and electro galvanized ULC-EG sheets meet the technical specification Sa < 1.0 µm as typical finishing for automotive panels[19] – the application which the sampled materials were manufactured for.

ISSN 1516-392X

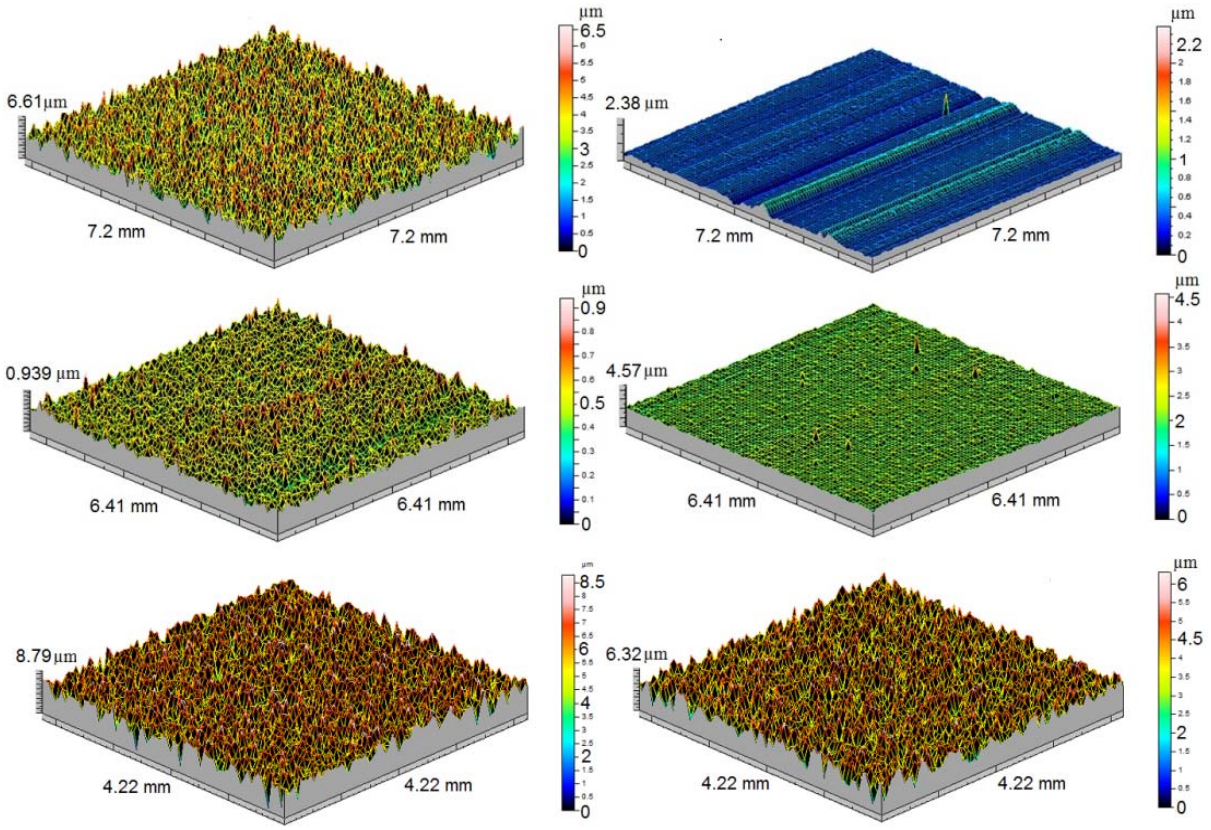

Figure2. Surface topography of samples before corrosion tests obtained by stylus profilometry: (a) as-received ULC steel; (b) metallographically ground and polished ULC steel; (c) plasma nitrided ULC-TPN steel; (d) Duplex-ULC steel; (e) galvanized ULC-GA; (f) electro galvanized ULC-EG.

Table 3. Surface parameters of samples before corrosion tests, obtained by stylus profilometry

Surface parameter (Gaussian filter, cut-off 0.8mm)			As-received ULC	Ground and polished ULC	Plasma nitrided ULC-TPN	Duplex-ULC	ULC-GA	ULC-EG
Amplitude parameters	S_a µm	Arithmetic average deviation	0.712	0.062	0.060	0.066	0.911	0.745
	S_q µm	Root mean square (RMS)	0.889	0.097	0.077	0.094	1.160	0.918
	S_p µm	Highest peak	3.20	1.94	0.433	2.48	3.73	2.56
	S_v µm	Deepest valley	3.42	0.44	0.51	2.10	6.34	3.76
	S_tµm	Max. total height	6.61	2.38	0.94	4.57	10.1	6.32
	S_zµm	Mean peak-to- valley height, 10 points	6.43	1.35	0.759	2.89	9.47	6.07
Statistic parameters	S_{ku}	Kurtosis	2.90	7.39	3.76	47.91	3.85	2.75
	S_{sk}	Skewness	-0.068	1.350	0.456	1.991	-0.736	-0.315

The measured inner and outer diameters of the wear scars resulting from calotest - as well as the calculated coating thickness - are resumed in Table 4. Three replicates were tested for each system.

ISSN 1516-392X

Table 4. Dimensions of the calotest wear scars after 1,350 rev, and calculated coating thickness

Sample	Mean inner diameter of the wear crater, *a* (x10^{-2} m)	Mean outer diameter of the wear crater, *b* (x10^{-2} m)	Average coating thickness *t* (x10^{-6} m)	Standard deviation of *t* (10^{-6} m)
Duplex-ULC	1482.9 ± 13.7	1582.0 ± 12.7	3.1	0.02
ULC-GA	1740.9 ± 20.4	2066.4 ± 17.1	12.4	0.13
ULC-EG	1738.2 ± 12.2	1942.3 ± 12.5	7.5	0.23

The XRD diffractogram and SEM photomicrographs of the ULC steel substrate are given in Figure3. It shows single ferrite phase (bcc α-Fe, ICDD 06-0696) with reasonably equiaxial grains. No other phase could be resolved by XRD for this ultra-low alloyed material.

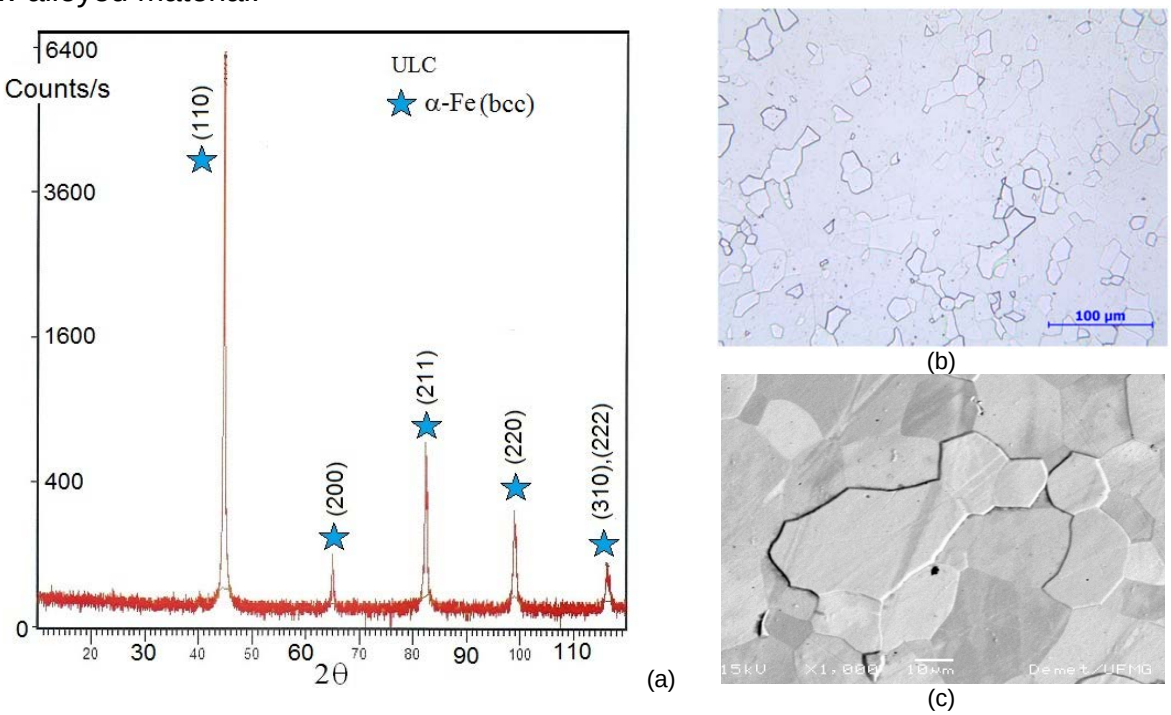

Figure3.ULC steel: (a) XRD results; (b) SEM photomicrograph, 2% Nital etching at 200 X, SE mode; and (c) SEM photomicrograph, 2% Nital etching at 1,000 X, BSE mode.

The diffractogram shown in Figure4 indicates that $Fe_{2-3}N$ (ε-hcp, ICDD 73-2102, 76-0090 and 86-0232) and Fe_4N (γ´-fcc, ICDD 86-0231) nitride phases were formed at the surface of the ferritic steel substrate as a consequence of plasma nitriding. These nitrides are relatively iron-rich with less than 35 at. % N.

As shown in Figure 5, after PAPVD coating a ternary nitride CrAlN film crystallized in a cubic NaCl B1 structure. It has a random orientation: diffraction peaks for (200), (111), (220) and other planes can be observed (ICDD 11-0065, 46-1200, 88-2360). The ε-$Fe_{2-3}N$ nitride - previously resolved in the nitrided material - could no longer be resolved at the surface of the Duplex-ULC: only the most iron-rich γ´- Fe_4N nitride was found. This is most probably a result of the decomposition of ε-$Fe_{2-3}N$ to γ´- Fe_4N during deposition of the coating, which is a thermal activated process. The CrAlN coating (approx. 3 µm thick) can be easily identified at the top of the fracture cross-section shown in the SEM photomicrographs (Figure 5). Just underneath the coating, the γ´- Fe_4N nitride phase grew - or segregated - as a succession of relatively wide

ISSN 1516-392X

needles, triangular in shape, up to 4 -5 µm long. A diffusion layer was formed underneath the nitride phase and all available nitrogen in this layer appears to be in solid solution.

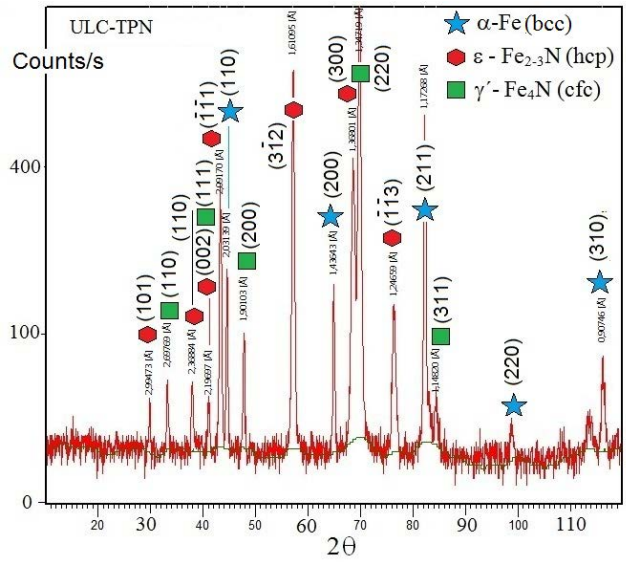

Figure 4. Diffractogram of the ULC-TPN steel sample, after plasma nitriding.

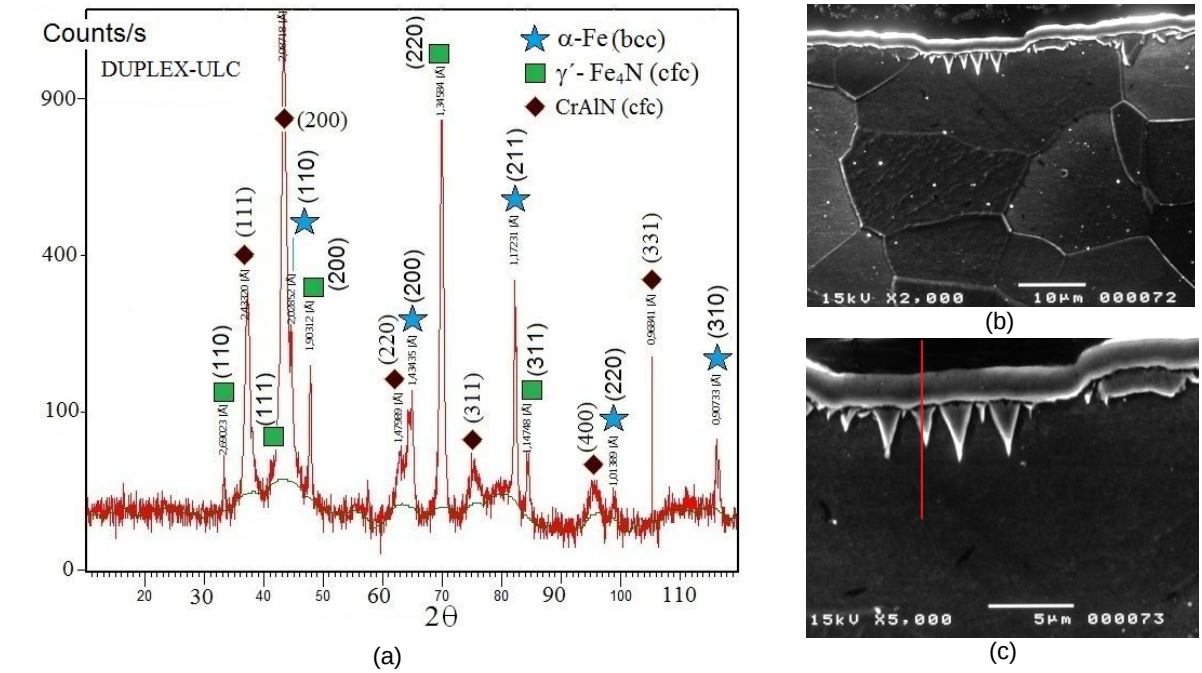

(a) (b) (c)

Figure5. Duplex-ULC: (a) XRD results; (b) SEM photomicrograph, cross-section, 2% Nital etching at 2000 X, SE mode; (c) SEM photomicrograph, cross-section, 2% Nital etching at 5,000 X, BSE mode.

During the galvannealing process for the UCL-GA, the cold-rolled steel sheet is coated with zinc on both sides by a continuous hot-dipping process. Immediately as the strip exits the coating bath, the zinc coating is subjected to an in-line heat treatment that converts the coating (approx. 12.4 µm) by inter-diffusion to Zn/Fe layers system. Depending on annealing temperature, annealing time, steel grade, aluminum content in the zinc pot and other parameters, different inter-metallic Zn/Fe phases are formed in the coating,[8,19–21] from substrate to surface: α-Fe (Ferrite); Γ (Fe_3Zn_{10}); Γ_1 (Fe_5Zn_{21} – Fe_4Zn_9); δ $FeZn_{10}$ ($FeZn_{11}$ – $FeZn_{6.67}$); ζ ($FeZn_{13}$); η Zn(Fe). The XRD diffractogram for ULC-GA is given in Figure6. From the α-Fe substrate to

ISSN 1516-392X

the surface a sequence of layers with progressively Zn-richer phases (Γ,δ, ζ, η-Zn) is formed.

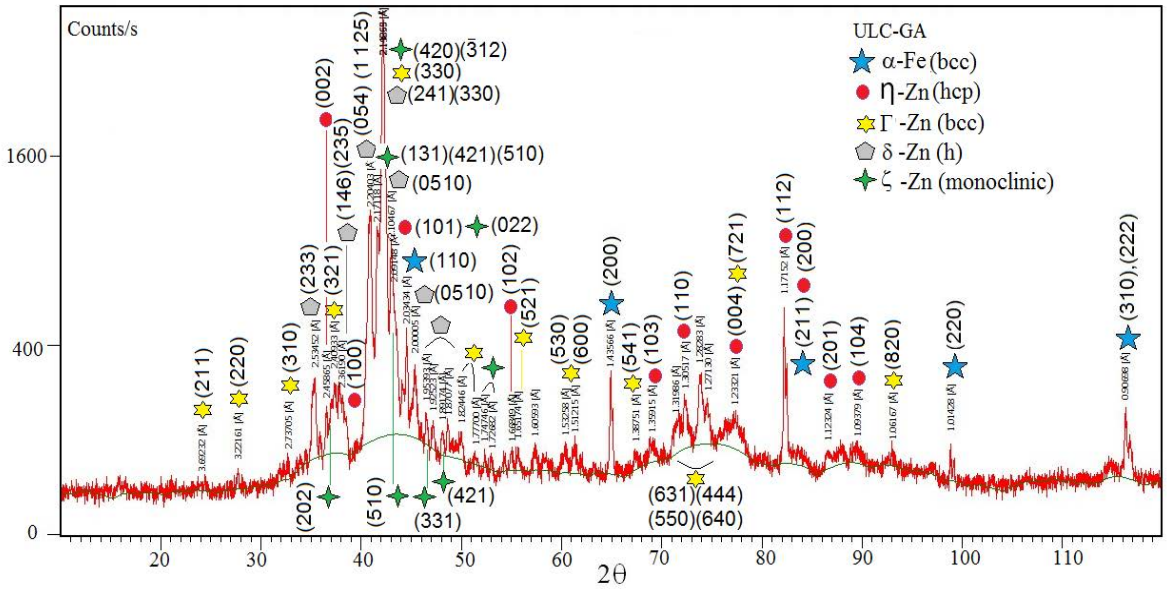

Figure 6. Diffractogram of the galvannealed sample ULC-GA.

The XRD diffractogram of the ULC-EG is shown in Figure7: coating is essentially pure η-Zn phase on top of the α-Fe steel substrate. The electro galvanized ULC-EG is manufactured by electro deposition of a pure Zn coating adhering on the steel substrate. Coating thickness is approx. 7.5 µm; as usually, it is thinner than the resulting from hot-dip galvanization.

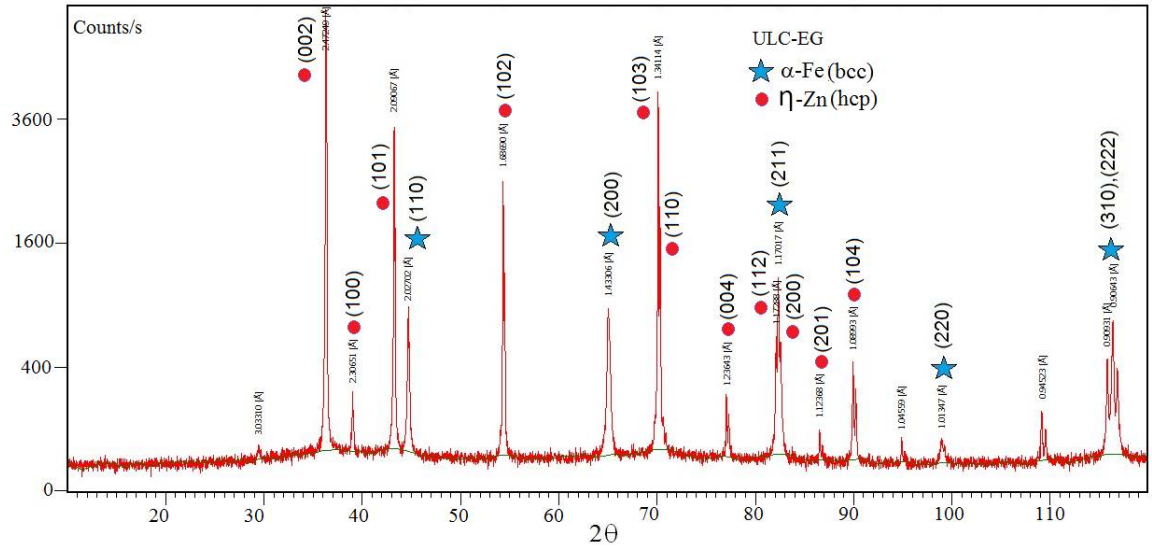

Figure 7. Diffractogram of the electro galvanized sample ULC-EG.

The comparative results from *OCP* and potentiodynamic anodic polarization tests are shown in Figure8. Numerical values for corrosion parameters are resumed in Table 5.

ISSN 1516-392X

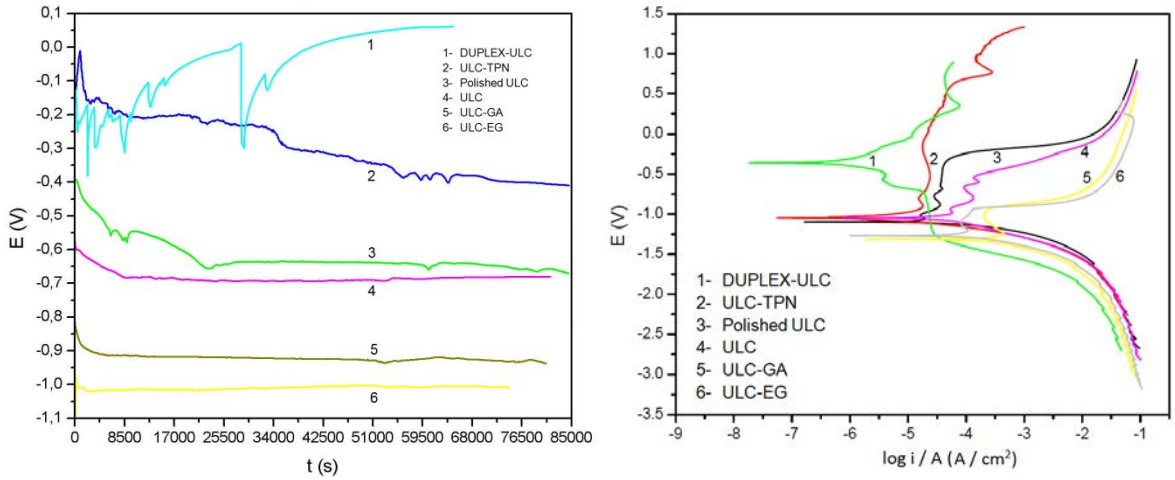

Figure8. Comparative results from: (a) *OCP*; (b) Potentiodynamic anodic polarization tests.

Table 5. Resulting parameters from corrosion tests in aerated 3.5% NaCl

Corrosion parameter	Unit	As-received ULC	Ground, polished ULC	Plasma nitrided ULC-TPN	Duplex-ULC	ULC-GA	ULC-EG
E_{OCP} after 24h	V	-0.69	-0.66	-0.42	+0.53	-0.94	-1.02
E_{corr}	V	-1.08	-1.13	-1.05	-0.34	-1.31	-1.26
I_{corr}	μA/cm^2	8.76	3.28	0.10	0.01	11.69	8.96
Rp	Ω.cm^2	951	2730	68465	505454	704	664
Corrosion mode after *PAP* tests	-	Severe general corrosion	Severe general corrosion	General corrosion, and pitting	Light general corrosion and pitting	Severe general corrosion, and pitting	Severe general corrosion, and pitting

The better corrosion resistance was obtained for the Duplex-ULC. The results for corrosion resistance could be correlated to the different nature in composition and morphology of the surfaces. ULC-GA samples showed Zn-Fe phases η - ζ - δ - Γ1 - Γ - αFe varying from surface to substrate; ULC-GE is pure η-Zn coating on ULC substrate; while the Duplex-ULC goes from a compact cfc-CrAlN coating to ε-$Fe_{2-3}N$ and γ´-Fe_4N nitrides within an α-Fe matrix with N in solid solution.

Results indicate that it is feasible to manufacture duplex Ti-stabilized ULC steel via DC-TPN and EB-PAPVD with actual improvement of the corrosion resistance. Potentiodynamic curves in Figure8 clearly showed a shift to higher corrosion potentials and lower corrosion current intensity from the untreated ULC substrate to the Duplex-ULC system. Based on the corrosion parameters, significant improvements in corrosion resistance were recorded for both nitrided and duplex-treated steels.

The literature[1,7,22] reports several facts supporting the high corrosion resistance of CrAlN coating, even higher than for other candidates as CrN, TiN or TiAlN. Even though, the coating may suffer from corrosive attack due to inherent coating defects (pores, cracks, columnar grains etc.) and inhomogeneities. Compared to CrN coating, CrAlN has usually less pores or defects[1] and forms a compact uniform barrier. TiN PVD coatings usually show a columnar structure, which may lead to straight grain boundaries and open (through coating) porosity, and therefore provides diffusion channels for the corrosive electrolyte to penetrate down to the substrate. While TiN based coatings usually show a strong (111) preferential orientation, the

ISSN 1516-392X

CrAlN show a random orientation with denser and finer and non-columnar microstructure. As a consequence, the corrosion resistance of the finer-structured coating/substrate system is improved.
Post-corrosion studies were conducted via SEM; Figure 9 shows SEM micrographs of corrosion damage in the samples after the potentiodynamic anodic polarization tests.

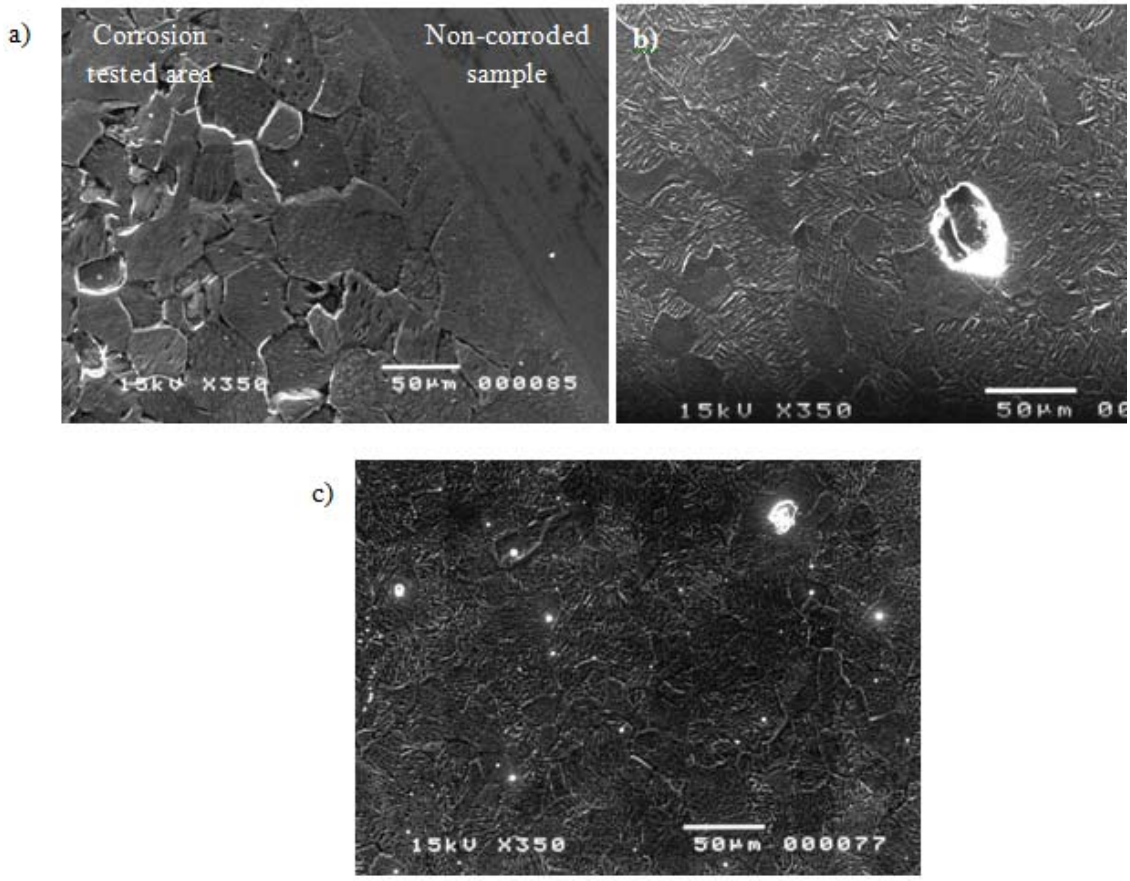

Figure 9. SEM micrographs of corrosion damage in the samples after the potentiodynamic anodic polarization tests: (a) ULC substrate; (b) plasma nitrided ULC-TPN; (c) Duplex-ULC.

Coating roughness should be minimized as much possible. The increased coating roughness would result in an increase of defects – could be both inclusions and pin-holes – in the coating which would consequently reduce the corrosion resistance of the coated system.[1,18] As can be seen from Table 3 and Figure2, the DC-TPN plasma nitriding followed by EB-PAPVD coating as used in this work is a fabrication route that essentially does not change the surface roughness of the substrate.
The low corrosion resistance of the galvanized systems – even compared to the untreated ULC substrate – can be understood by the sacrificial properties of the Zn coating.[8,11,12,22] In the galvanic series, the standard potential for Zinc (E^0 = -0.762 V) is less noble than for α-Fe (E^0 = -0.477 V), as in most environments and ambient temperatures. Zn coatings add corrosion resistance to steel by galvanic protection, acting as a sacrificial anode to protect the underlying steel at voids, scratches, and cut edges of the sheet. The galvanized ULC-GA and ULC-EG systems showed the lowest corrosion resistance properties, as should be expected from the sacrificial approach of the Zn-based coatings. Severe corrosion and pitting were observed after the potentiodynamic polarization tests.

ISSN 1516-392X

The reduction of surface roughness of the ULC substrate by grinding and polishing lead to a reduction in the corrosion current, as can be seen when comparing data from Tables 3 and 5. The lower roughness parameters (*Sa*, *Sq* etc.)allowed an increase in corrosion protection efficiency. However, the E_{corr} values are very similar for the as received and for the mirror polished substrate, both having the same chemical nature. Despite the latter seems to be more resistant to atmospheric corrosion, severe general corrosion was observed in post-corrosion SEM studies for both substrate samples after *PAP* tests (Figure9a). Plasma nitrided ULC-TPN sample suffered general corrosion and pitting (Figure9b), with corrosion parameters indicating lower corrosion resistance than for the Duplex-ULC. The results from the potentiodynamic tests clearly indicate that the Duplex treatment was the most effective method to enhance the corrosion resistance of ULC steel. Light general corrosion and a few pits were observed in the post-corrosion studies of Duplex-ULC (Figure9c).

4 CONCLUSIONS

Under the experimental conditions of the present study, the results for corrosion resistance can be correlated to the different nature in composition and morphology of the surfaces. ULC-GA samples showed Zn-Fe phases η - ζ - δ - Γ1 - Γ - αFe varying from surface to substrate; ULC-GE is pure η-Zn coating on ULC substrate; while the Duplex-ULC goes from a compact cfc-CrAlN coating to ε-$Fe_{2\text{-}3}N$ and γ´-Fe_4N nitrides within an α-Fe matrix with N in solid solution. The CrAlN coating shows a randomly orientated microstructure, apparently free of through-coating defects.
Based on the E_{OCP}, E_{corr}, I_{corr}, *Rp* and η_c values, the Duplex-ULC showed the highest corrosion resistance. Plasma nitriding was second in corrosion resistance, with a more negative E_{corr} value. The galvannealed ULC-GA show the lowest corrosion resistance. The ULC substrate – either as received or as ground and polished – is more corrosion resistant than the Zn-coated ULC-GA and ULC-GE steels. The reduction in surface roughness was beneficial for improving corrosion resistance of the untreated substrate. Results indicate that it is feasible to manufacture duplex Ti-ULC steel via DC-TPN and EB-PAPVD with actual improvement of the corrosion resistance. Potentiodynamic curves clearly showed a shift to higher corrosion potentials and lower corrosion current intensity from the untreated ULC substrate to the duplex system. While the Zn-based coatings intend a sacrificial galvanic protection, the CrAlN coating provides higher intrinsic corrosion resistance of the steel substrate. Duplex treatment clearly was the most effective method to enhance the corrosion resistance of ULC steel.

Acknowledgments

The authors would like to express their acknowledgments to the School of Engineering and Metallurgical Department from UFMG (Demet-UFMG), the Mechanical Department from UFES (DEM-UFES), Usiminas. S.A., and the Center for Development of Nuclear Technology (CDTN – MG) for their extensive support and effective co-operation.

ISSN 1516-392X

REFERENCES

1 X. Ding et al. Corrosion resistance of CrAlN and TiAlN coatings deposited by lateral rotating cathode arc Thin Solid Films 516 (2008) 5716–5720.
2 K. Abotani et. al. Hot-dip galvanized sheet steel with excellent press formability and surface quality for the automotive panels. Kawasaki Steel Technical Report No. 48 (2003),17 p.
3 A. Matthews; A. Leyland. Hybrid Techniques in surface engineering. Surface and Coatings Technology 71 (1995) 88-92.
4 A. Spain et. al. Characterization and applications of Cr-Al-N coatings. Surface & Coatings Technology 200 (2005), pp. 1507 – 1513.
5 J. C. Avelar-Batista et. al. Triode plasma nitriding and PVD coating: A successful pre-treatment combination to improve the wear resistance DLC coatings on Ti6Al4V. Surface & Coatings Technology 201 (2006) 4335–4340.
6 A. J. Abdalla; V. H. Baggio-Scheid. Tratamentos termoquímicos a plasma em aços carbono. Corros. Prot. Mater., Vol. 25 N.º 3 (2006), pp. 92- 96.
7 J. Lin, B. Mishra, et. al. Effects of the substrate to chamber wall distance on the structure and properties of CrAlN films deposited by pulsed-closed field unbalanced magnetron sputtering (P-CFUBMS). Surface & Coatings Technology 201 (2007), pp. 6960–6969.
8 A. R. Marder. The metallurgy of zinc-coated steel. Progress in Materials Science 45 (2000), pp. 191-271.
9 H. Hadzima et. al. Microstructure and Corrosion Properties of Ultrafine-Grained Interstitial Free Steel. Materials Science and Engineering A 462 (2007), pp. 243–247.
10 M. B. Kannan; R. K. S. Raman; S. Khoddam. Comparative studies on the corrosion properties of a Fe–Mn–Al–Si steel and an interstitial-free steel. Corrosion Science 50 (2008), pp. 2879–2884.
11 M. E. P. Souza et. al. Comparative behavior in terms of wear and corrosion resistance of galvanized and zinc-iron coated steels. RevistaMatéria, V. 12, No.4 (2007), p. 618-23.
12 R. J. A. Marques. Avaliação da Resistência à Corrosão de Aços IF Revestidos com Zinco e Ligas de Zinco-Ferro Destinados à Indústria Automobilística. Dissertação de Mestrado em Engenharia Metalúrgica e de Minas PPGEM - UFMG, 2008.
13 A. J. Abdalla et. al. Melhoria nas propriedades de um aço de baixo carbono tratado termoquimicamente a plasma. 8º CONGRESO IBEROAMERICANO DE INGENIERIA MECANICA. 2007, 10p.
14 A. J. Abdalla et. al. Resistência à corrosão em aços de baixo carbono tratados termoquimicamente a plasma. Revista Brasileira de Aplicações de Vácuo, Vol. 23, No. 1 (2004), pp. 5-10.
15 B. C. Ferreira; M. A. S de Oliveira. Tratamento termoquímico a plasma de aço-carbono. Boletim Técnico Petrobras. Rio de Janeiro 46 (1/2). 2003, pp. 167 - 176.
16 ASTM G5-94. Standard Reference Test Method for Making Potentiostatic and Potentiodynamic Anodic Polarization Measurements. 2004, 12p.
17 K. L. Rutherford; I. M. Hutchings. A micro-abrasive wear test, with particular application to coated systems. Surface and Coatings Technology 79 (1996) pp. 231-239.
18 M. G. Gee, A. Gant; I. M Hutchings. Ball cratering or micro-abrasion wear testing of coatings. Measurement Good Practice Guide No. 57, November 2002. ISSN: 1368-6550, http://publications.npl.co.uk.
19 M. H. Hong. Correlation between the microstructure of galvannealed coatings and of the defoliation during press forming. ISIJ International, Vol. 45, No. 6 (2005) pp. 896 – 902.
20 J. M. Long et. al. Characterization of galvanneal coatings on strip steel. Materials Forum, Vol. 27 (2004) pp. 62 - 67.
21 S. Wienströer. International Centre for Diffraction Data - Advances in X-ray Analysis. Zinc/Iron phase transformation studies on galvannealed steel coatings by X-Ray diffraction. JCPDS - ICDD Advances in X-ray Analysis, Vol. 46 (2003), pp. 291 – 296.
22 H. C. Barshilia et. al. A comparative study of reactive direct current magnetron sputtered CrAlN and CrN coatings. Surface & Coatings Technology 201 (2006) pp. 2193–2201.